

NACA TN 4352

# NATIONAL ADVISORY COMMITTEE FOR AERONAUTICS

TECHNICAL NOTE 4352

TABLES AND GRAPHS OF NORMAL-SHOCK PARAMETERS  
AT HYPERSONIC MACH NUMBERS AND  
SELECTED ALTITUDES

By Paul W. Huber

Langley Aeronautical Laboratory  
Langley Field, Va.



Washington

September 1958



TECHNICAL NOTE 4352

TABLES AND GRAPHS OF NORMAL-SHOCK PARAMETERS

AT HYPERSONIC MACH NUMBERS AND

SELECTED ALTITUDES

By Paul W. Huber

SUMMARY

Tables and graphs of normal-shock parameters are presented for real air in thermal and chemical equilibrium at conditions ahead of the shock corresponding to six selected altitudes, and for temperatures behind the shock from  $2,000^{\circ}$  K to  $11,000^{\circ}$  K. The altitudes used are those representing the boundaries of the isothermal layers in that part of the earth's atmosphere considered applicable to aerodynamic flight; that is, below an altitude of 300,000 feet. The altitude data and the real-air thermodynamic data used are reliable for application to this range of altitudes. Tabulated values at each altitude as a function of the temperature behind the shock are presented of the normal-shock Mach numbers, flight velocity, enthalpy behind the shock, and ratios of real to ideal values of pressure, density, temperature, and velocity of sound. Graphs are presented to show the variation of the normal-shock parameters with flight Mach number and altitude, and some discussion of the dependence of the parameters on the initial pressure and temperature is given. A method for adapting the data to the case of oblique shocks is included.

INTRODUCTION

It can be shown from the tabulated thermodynamic properties for real air (for example, ref. 1) and the Rankine-Hugoniot shock relations that the hypersonic shock parameters are strongly dependent upon both temperature and pressure as well as on Mach number. This concept is in contrast to that for ideal air in which no temperature or pressure dependency is indicated because of the assumed constancy of the specific heats, constancy of the molecular weight, and perfectness of the gas. (See, for example, ref. 2.) Until the relatively recent advent of hypersonic flight in the atmosphere, the assumption of near ideal air has been adequate for flight, since the temperatures encountered were moderate and hence the thermal properties of the air were near to the ideal values. At high temperatures, however, the thermal properties of

air become greatly different from those of ideal air, and, in fact, the air changes composition due to dissociation and ionization of the constituent particles.

A number of real-air hypersonic shock computations have been published in recent years (refs. 3 to 8) in which the latest accepted thermodynamic air data (9.758 electron volts for the dissociation energy of nitrogen molecules) are used. In general, however, either outdated altitude information was used, or the conditions ahead of the shock were specified in terms of independent values of temperature and pressure. The latter is very useful for general application to hypersonic tunnel work, but since the atmosphere involves a rather definite combination of pressure and temperature at each altitude, interpolation of the data to conditions corresponding to a given altitude is often cumbersome. This inconvenience arises from the double interpolation required to correct for initial temperature and pressure, whereas certain of the functions are strongly, but not linearly, dependent on temperature or pressure (or both) in the hypersonic atmospheric regime.

In order to provide values of the normal-shock parameters which are directly applicable to the selected altitudes, the computations presented are based upon reliable thermodynamic information for high-temperature argon-free air (ref. 1) and atmospheric conditions at altitudes up to 300,000 feet (refs. 9 and 10). This range of altitudes encompasses that part of the earth's atmosphere in which flight where aerodynamic forces are used to advantage is generally considered. It may be noted that more recent higher altitude atmosphere data from earth satellites have superseded the model atmosphere of reference 10 for altitudes above 450,000 feet, but in the range of altitudes used herein there has been no significant change. Reference 10 should, therefore, still represent the best available data. The computations are based on complete thermal and chemical equilibrium, and it is to be remembered that thermal relaxation and reaction rate phenomena in hypersonic flow will, in some cases, restrict the usefulness of such computations. References 11 and 12 contain discussions of possible effects attributable to these nonequilibrium phenomena.

#### SYMBOLS

H	geopotential altitude, ft (defined in refs. 9 and 10)
u	fluid velocity, ft/sec
h	specific enthalpy, $\frac{\text{ft}^2}{\text{sec}^2}$

- p absolute pressure, lb/sq ft abs
- V molal volume based on undissociated mole,  $\frac{m_0}{m} \frac{RT}{p}$ ,  $\frac{\text{ft}^3}{\text{slug-mole}}$
- T absolute temperature, °K or °R, as required
- a velocity of sound, ft/sec
- M Mach number,  $u/a$
- K ratio of real-gas parameter to ideal-gas parameter for same value of  $M_1$ , where the particular parameter is indicated by a subscript (for example,  $K_{\rho 2} = \frac{\rho_2}{\rho_{2,i}}$ )
- m molecular weight,  $\frac{\text{slugs}}{\text{slug-mole}}$
- R universal gas constant,  $\frac{\text{ft-lb}}{\text{slug-mole-}^\circ\text{K}}$
- $\delta$  flow-deflection angle
- $\rho$  mass density,  $m_0/V$ , slugs/cu ft
- $\theta$  oblique-shock angle
- $\gamma$  ratio of specific heats
- Subscripts:
- 0 at standard sea-level pressure (2,116 lb/sq ft abs); at temperature of 273.16° K
- 1 at altitude conditions and ahead of normal shock
- 2 behind normal shock
- i ideal air ( $\gamma = 1.40$ ;  $m = m_0$ ;  $\frac{pV}{RT} = 1.0$ )
- $\theta$  at altitude conditions and ahead of oblique shock
- $\delta$  deflected flow behind oblique shock

## METHOD OF COMPUTATION

The equations denoting conservation of mass, momentum, and energy are written for the case of a normal shock wave in the following equations:

$$\rho_1 u_1 = \rho_2 u_2 \quad (1)$$

$$p_1 + \rho_1 u_1^2 = p_2 + \rho_2 u_2^2 \quad (2)$$

$$h_1 + \frac{1}{2} u_1^2 = h_2 + \frac{1}{2} u_2^2 \quad (3)$$

The ideal-gas relations for the equation of state at the reference conditions and the velocity of sound on the low-pressure side (ahead of the shock) are:

$$\left. \begin{aligned} \frac{p_0}{\rho_0} &= \frac{R}{m_0} T_0 \\ a_1^2 &= \gamma_1 \frac{p_1}{\rho_1} \end{aligned} \right\} \quad (4)$$

since the gas is very nearly ideal at these conditions.

If equations (1), (2), (3), and (4) are combined, the following relations are obtained:

$$\left( \frac{p_2}{p_0} - \frac{p_1}{p_0} \right) \left( \frac{1}{\rho_1} + \frac{1}{\rho_2} \right) = 2 \left( \frac{h_2}{\frac{R}{m_0} T_0} - \frac{h_1}{\frac{R}{m_0} T_0} \right) \quad (5)$$

$$M_1^2 = \frac{1}{\gamma_1} \frac{\rho_2}{\rho_1} \frac{\frac{p_2}{p_1} - 1}{\frac{\rho_2}{\rho_1} - 1} = \left( \frac{u_1}{a_1} \right)^2 \quad (6)$$

Equation (5) is in a form suitable for insertion of tabulated values of the thermodynamic properties for real air and of the ambient-air properties at selected altitudes. Solution of equation (5) is obtained by

specifying values of  $T_2$ ,  $\frac{p_1}{p_0}$ ,  $\frac{\rho_1}{\rho_0}$ , and  $\frac{h_1}{\frac{R}{m_0} T_0}$  and iterating by using

interpolated values of the tabulated thermodynamic properties -  $\frac{p_2}{p_0}$ ,  $\frac{\rho_2}{\rho_0}$ , and  $\frac{h_2}{\frac{R}{m_0} T_0}$  at the specified value of  $T_2$  until the equation is

satisfied. Interpolation of these tabulated air properties is accurately accomplished by linear interpolation of the logarithms of the values. Iteration of equation (5) is made rapidly convergent by first choosing two sets of the tabulated properties and plotting values of the left and right sides of the equation as a function of  $\frac{p_2}{p_0}$  for these two cases and

finding a straight-line intersection. This intersection is generally very close to the final solution for  $\frac{p_2}{p_0}$ . Values of  $M_1$  and  $u_1$  are then found directly from equation (6) by using values of  $\gamma_1$  and  $a_1$  for argon-free air. In order to present the Mach number and velocity of sound behind the normal shock, values of  $\frac{a_2}{a_0}$  pertinent to each solu-

tion  $\left( \frac{h_2}{\frac{R}{m_0} T_0} \text{ and } T_2 \right)$  were read from a large chart available in reference 6. This chart is based on computations of  $a_2$  from reference 13 and represents the case of complete thermal and chemical equilibrium. The ratios  $M_2$  and  $\frac{a_2}{a_1}$  were then computed by using  $\frac{u_2}{u_1}$  from equation (1) and  $\frac{a_2}{a_0}$  along with values of  $\frac{a_1}{a_0}$  for each altitude.

#### ACCURACY

In the iteration of equation (5) it was arbitrarily decided that the accepted solution would require at least 0.2 percent agreement between the values for the left and right sides of the equation. Inspection of equations (5) and (6) and of the thermodynamic data shows that this requirement establishes a similar accuracy for  $p_2$  and  $\rho_2$ , with the value of  $M_1$  from equation (6) being within 0.1 percent of the correct value. Justification for this seeming crudeness lies mainly in the strong dependence of the results on the altitude data, which are certainly

not available for application to a given flight case to any greater accuracy. Some justification also may be found as a result of the use of argon-free-air data, which may be of the order of 1 percent different from atmospheric air in the enthalpy-temperature relation, although the errors resulting in the relations of the nondimensional aerodynamic parameters (for example,  $\frac{p_2}{p_1} = f(M_1)$ ) should be less than 1 percent.

#### DATA INPUT

Values of the parameters  $\frac{p_2}{p_0}$ ,  $\frac{\rho_2}{\rho_0}$ ,  $\frac{h_2}{\frac{R}{m_0} T_0}$ , and  $T_2$  were taken from

reference 1 and represent equilibrium values of the properties including effects of dissociation and ionization for an assumed argon-free real air. A somewhat more complete tabulation of the real-air thermodynamic properties may be found in reference 13 with the values being essentially in agreement with those of reference 1. Tabulated air properties may also be found in reference 14. Values of the parameters  $T_1$ ,  $\frac{p_1}{p_0}$ , and  $\frac{\rho_1}{\rho_0}$  as functions of  $H$  were taken from data given in references 9 and 10 and represent a reliable model of the upper atmospheric conditions for the range of altitudes applicable to aerodynamic flight.

Values of  $\frac{h_1}{\frac{R}{m_0} T_0}$  and  $\frac{a_1}{a_0}$  were taken from reference 15 for conditions corresponding to each altitude.

Computations of the shock parameters are included for the range of temperatures  $T_2$  from 2,000° K to 11,000° K at the intervals found in reference 1, for each altitude chosen. The altitudes chosen were those below 300,000 feet which represent boundaries of the isothermal layers within this region of the earth's atmosphere as taken from references 9 and 10. These altitudes and a few others are listed in table I and pertinent information for use in the computations is also shown in table I and plotted in figures 1 and 2.

Only these six altitudes were selected because it was desirable to limit the computations to a minimum number of cases. Since the temperature variation with altitude in the atmosphere is so peculiarly non-monotonic (see fig. 1), selection of the discontinuous points with the rather linear variation between these points allows for possible interpolation of such functions as may exhibit relationships that are largely



temperature dependent. The data of figure 2 indicate that solely pressure-dependent functions may be logarithmically interpolated to other altitudes to a reasonable degree.

## RESULTS

The results of the computations are given in table II for each altitude as a function of the temperature  $T_2$  behind the normal shock. The tabulated values include the parameters  $\frac{p_2}{p_1}$ ,  $\frac{\rho_2}{\rho_1}$ ,  $M_1$ ,  $u_1$ ,  $\frac{T_2}{T_1}$ ,

$\frac{h_2}{\frac{R}{m_0} T_0}$ ,  $\frac{a_2}{a_1}$ , and  $M_2$ . Also tabulated are the ratios of these real-air

parameters to the corresponding ideal-air parameters,  $K_{p2}$ ,  $K_{\rho 2}$ ,  $K_{T2}$ ,  $K_{a2}$ , and  $K_{M2}$ , for the same value of  $M_1$  (ideal parameters are independent of  $p_1$  and  $T_1$  and therefore of  $H$ ). The ideal-air normal-shock parameters are computed from the relations found in reference 2 by use of  $\gamma_1 = 1.400$ . Plotted in figures 3 to 7 are the ratios  $K_{p2}$ ,  $K_{\rho 2}$ ,  $K_{T2}$ ,  $K_{a2}$ , and  $K_{M2}$  as functions of  $M_1$  for each altitude. The values of  $a_2$  and consequently of  $M_2$  given in the tables and figures are listed only within the range of data contained in the chart of reference 6.

Marked departures of the real-air normal-shock parameters from the ideal-air values are shown to occur in these figures with  $K$  being as low as 0.17 and as high as 3.5. In general, the nonideality of the results increases with flight Mach number and altitude - this being physically a result of the large increase of the heat capacity of the gas with temperature (Mach number) and the large increase of degree of dissociation with the inverse of pressure (altitude) at these temperatures. The peculiar nonlinearity of the results when plotted as a function of Mach number is largely due to the dissociation at different energy levels of oxygen and nitrogen and when plotted as a function of altitude is due also to the peculiar variation of temperature in the atmosphere (fig. 1). It is obvious that interpolation or extrapolation, even of altitude results such as these, should be attempted with extreme caution.

For purposes of interpolation to other altitudes, however, it can be shown from table II (and from examination of the shock equations) that certain parameters will exhibit less sensitivity to the real-air effects than others. For example, the shock pressure ratio  $p_2/p_1$  as a

function of Mach number  $M_1$  has a relatively slight dependence on initial pressure and temperature, whereas this parameter as a function of  $u_1$  shows a strong dependence on the initial temperature  $T_1$  but again little or no dependence on initial pressure  $p_1$ . The shock density ratio  $\rho_2/\rho_1$  shows only a slight dependence on initial temperature when plotted as a function of flight velocity  $u_1$  but has a definite dependence on initial pressure; however, when plotted as a function of  $M_1$ , the shock density ratio shows appreciable dependence on both temperature and pressure. For another example, use of the shock temperature ratio  $T_2/T_1$  as a parameter introduces a strong dependence on the initial temperature  $T_1$ , whether it be plotted as a function of flight velocity or Mach number, whereas if shock temperature rise  $T_2 - T_1$  or  $T_2$  is used, this temperature dependency is greatly reduced, particularly when plotted against  $u_1$ . A pressure dependency, however, is seen in all cases. In general, by judicious use of the shock parameters, altitude interpolation is possible to a reasonable degree of accuracy for many engineering applications.

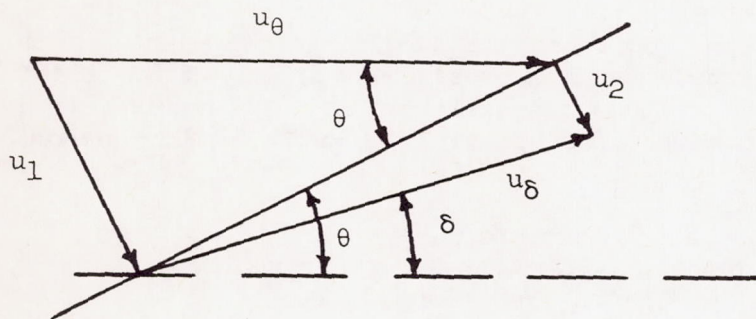
As an aid in interpolation of these results to other altitudes, therefore, the parameters  $K_{\rho 2}$  and  $T_2$  are plotted as a function of flight velocity  $u_1$  in figures 8 and 9, respectively. For use with these figures the atmospheric velocity of sound  $a_1$ , calculated by using equation (4), is shown as a function of altitude  $H$  in figure 10 for readily finding the value of  $u_1 = M_1 a_1$  at any desired altitude and Mach number.

It is seen in figures 1 and 2 that the altitude data from reference 10, which are considered to be the most applicable data to aerodynamic flight in the atmosphere, are significantly different from the older data (ref. 16) at altitudes above 82,000 feet and are much closer to the data of reference 17. This comparison indicates that normal-shock computations based on the older data (for example, ref. 6) would also be different above this altitude. Differences of as high as 25 percent may be noted in values of  $p_2/p_1$  or  $T_2/T_1$  plotted against  $u_1$ .

One exception is noted to the differences that may occur above 82,000 feet and that is that the altitude data at 120,000 feet used for the computations of reference 6 are very close to the later altitude data (see figs. 1 and 2). In order, therefore, to provide an additional altitude on figures 3 to 7, the curves for an altitude of 120,000 feet from reference 6 have been read and replotted to these coordinates.

A word may be said about the stagnation-point values in the flow behind the shock wave. Computations of these values have not been included in the report for two reasons; first, the change in flow values from behind the normal shock to the stagnation point is relatively small, and second, where such values may be required, the computation is readily made by using table II along with a large Mollier type chart such as is obtained from reference 6. With regard to the first reason, it can be shown from inspection of the energy equation applied to this case, together with a few sample computations in the hypersonic range, that the temperature rise at stagnation behind the normal shock is of the order of 1 percent and that the density and pressure rise are of the order of 5 percent.

Values of the oblique-shock parameters, although not included in the present analysis, may be readily computed from the normal-shock parameters found in table II along with the oblique-shock relations illustrated in the following sketch:



These parameters are:

$$\sin \theta = \frac{u_1}{u_\theta} = \frac{M_1}{M_\theta} \quad (7)$$

$$\frac{\tan(\theta - \delta)}{\tan \theta} = \frac{u_2}{u_1} = \frac{1}{\rho_2/\rho_1} \quad (8)$$

$$\sin(\theta - \delta) = \frac{u_2}{u_\delta} = \frac{M_2}{M_\delta} \quad (9)$$

For each desired altitude and flight velocity  $u_0$  (or  $M_0$ ):

(1) Assume values of  $u_1$  (or  $M_1$ ) as listed in table II, and read corresponding values of  $\rho_2/\rho_1$ ,  $p_2/p_1$ , and so on.

(2) Find  $\theta$  from equation (7),  $\delta$  from equation (8), and  $u_8$  from equation (9).

#### CONCLUDING REMARKS

Normal-shock parameters for real air in thermal and chemical equilibrium have been presented in both tabular and graphical form for six selected altitudes for the range of temperatures behind the shock from  $2,000^\circ\text{K}$  to  $11,000^\circ\text{K}$ . Reliable altitude and thermodynamic air data for application to aerodynamic flight in the atmosphere have been used. The graphs serve to illustrate the variation of the normal-shock parameters with Mach number and altitude. The dependence of the parameters on initial temperature and pressure is indicated so that interpolation of the parameters to other altitudes may be readily carried out. Included is a method for adapting the data to the case of oblique shocks.

Langley Aeronautical Laboratory,  
National Advisory Committee for Aeronautics,  
Langley Field, Va., June 9, 1958.

## REFERENCES

1. Hilsenrath, Joseph, and Beckett, Charles W.: Tables of Thermodynamic Properties of Argon-Free Air to 15,000° K. AEDC-TN-56-12, Arnold Eng. Dev. Center, Sept. 1956. (Also available from ASTIA as Doc. No. AD-98974.)
2. Ames Research Staff: Equations, Tables, and Charts for Compressible Flow. NACA Rep. 1135, 1953. (Supersedes NACA TN 1428.)
3. Bond, J. W., Jr.: Equilibrium Conditions Behind a Normal Shock Front in the Atmosphere. MSD 1456, Lockheed Aircraft Corp., Dec. 20, 1955. (Available from ASTIA as AD-113496.)
4. Romig, Mary F.: The Normal-Shock Properties for Air in Dissociation Equilibrium. Jour. Aero. Sci., (Readers' Forum), vol. 23, no. 2, Feb. 1956, pp. 185-186.
5. Moeckel, Wolfgang E.: Oblique-Shock Relations at Hypersonic Speeds for Air in Chemical Equilibrium. NACA TN 3895, 1957.
6. Feldman, Saul: Hypersonic Gas Dynamic Charts for Equilibrium Air. AVCO Res. Lab., Jan. 1957.
7. Hochstim, Adolf R.: Gas Properties Behind Shocks at Hypersonic Velocities. I. Normal Shocks in Air. Rep. No. ZPh(GP)-002, Convair, Jan. 30, 1957.
8. McKowen, Paul: The Equilibrium Composition and Flow Variables for Air Dissociated by a Strong Shock Wave. Rep. No. 02-984-040, Bell Aircraft Corp., Mar. 8, 1957.
9. Anon.: Standard Atmosphere - Tables and Data for Altitudes to 65,800 Feet. NACA Rep. 1235, 1955. (Supersedes NACA TN 3182.)
10. Minzner, R. A., and Ripley, W. S.: The ARDC Model Atmosphere. Air Force Surveys in Geophysics No. 86 (AFCRC TN-56-204), Geophysics Res. Dir., Air Force Res. Center (Bedford, Mass.), Dec. 1956. (Available as ASTIA Doc. 110233.)
11. Feldman, Saul: The Chemical Kinetics of Air at High Temperatures: A Problem in Hypersonic Aerodynamics. Res. Rep. 4, AVCO Res. Lab., Feb. 1957. (Formerly Res. Note 25.)
12. Resler, E. L., Jr.: Characteristics and Sound Speed in Nonisentropic Gas Flows With Nonequilibrium Thermodynamic States. Jour. Aero. Sci., vol. 24, no. 11, Nov. 1957, pp. 785-790.

13. Logan, J. G., Jr., and Treanor, C. E.: Tables of Thermodynamic Properties of Air From 3,000° K to 10,000° K at Intervals of 100° K. Rep. No. BE-1007-A-3. Cornell Aero. Lab., Inc., Jan. 1957.
14. Gilmore, F. R.: Equilibrium Composition and Thermodynamic Properties of Air to 24,000° K. U. S. Air Force Project RAND Res. Memo. RM-1543, The RAND Corp., Aug. 24, 1955. (Also available from ASTIA as AD 84052.)
15. Hilsenrath, Joseph, Beckett, Charles W., et al.: Tables of Thermal Properties of Gases. NBS Cir. 564, U. S. Dept. Commerce, 1955.
16. Anon.: Handbook of Supersonic Aerodynamics. NAVORD Rep. 1488 (vol. 1) Bur. Ord., Apr. 1, 1950.
17. The Rocket Panel: Pressures, Densities, and Temperatures in the Upper Atmosphere. Phys. Rev., vol. 88, no. 5, Second ser., Dec. 1, 1952, pp. 1027-1032.

TABLE I.- ATMOSPHERIC ALTITUDE CONDITIONS AS TAKEN  
FROM REFERENCES 9 AND 10

H, ft	T <sub>1</sub> , °K	$\frac{p_1}{p_0}$	$\frac{\rho_1}{\rho_0}$	$\frac{a_1}{a_0}$	$\frac{h_1}{\frac{R}{m_0} T_0}$
0	288	1.00	0.9474	1.0272	3.68
36,000	217	.2243	.2824	.8905	2.77
82,020	217	$.2456 \times 10^{-1}$	$.3095 \times 10^{-1}$	.8905	2.77
120,000	251	$.4518 \times 10^{-2}$	$.4910 \times 10^{-2}$	.9591	3.21
154,200	283	$.1189 \times 10^{-2}$	$.1148 \times 10^{-2}$	1.0174	3.61
173,885	283	$.5756 \times 10^{-3}$	$.5559 \times 10^{-3}$	1.0174	3.61
246,060	197	$.2420 \times 10^{-4}$	$.3356 \times 10^{-4}$	.8484	2.51
295,280	197	$.1792 \times 10^{-5}$	$.2485 \times 10^{-5}$	.8484	2.51

Constants for argon-free air are (ref. 1):

$p_0 = 2,116 \text{ lb/sq ft}$ $T_0 = 273.16^\circ \text{ K}$ $\rho_0 = 0.002499 \text{ slug/cu ft}$ $a_0 = 1,089 \text{ ft/sec}$	$m_0 = 28.86 \frac{\text{slugs}}{\text{slug-mole}}$ $\gamma_1 = 1.400$ $\frac{R}{m_0} T_0 = 847,100 \frac{\text{ft}^2}{\text{sec}^2}$
--	---





TABLE II.- HYPERSONIC NORMAL-SHOCK PARAMETERS AT SIX SELECTED ALTITUDES - Continued

$T_2$ , °K	$\frac{P_2}{P_1}$	$\frac{\rho_2}{\rho_1}$	$M_1$	$u_1$ , ft	$\frac{T_2}{T_1}$	$\frac{h_2}{R_{M_0} T_0}$	$\frac{a_2}{a_1}$	$M_2$	$K_{P2}$	$K_{\rho 2}$	$K_{T2}$	$K_{a2}$	$K_{M2}$
H = 154,200 ft; $T_1 = 283^\circ$ K; $p_1 = 0.1189 \times 10^{-2}$ atm.													
2,000	43.72	6.178	6.032	$6.683 \times 10^3$	7.067	29.29	-----	-----	1.0341	1.1713	0.8818	-----	-----
2,200	50.31	6.454	6.454	7.151	7.774	33.11	-----	-----	1.0389	1.2048	.8600	-----	-----
2,400	58.43	6.836	6.929	7.677	8.481	37.69	-----	-----	1.0462	1.2580	.8252	-----	-----
2,600	68.97	7.374	7.492	8.301	9.187	43.55	-----	-----	1.0560	1.3384	.7750	-----	-----
2,800	82.69	8.070	8.158	9.038	9.894	51.09	-----	-----	1.0672	1.4460	.7126	-----	-----
3,000	99.66	8.856	8.910	9.872	10.601	60.45	3.047	0.3302	1.0780	1.5690	.6472	0.7528	0.8467
3,200	119.34	9.652	9.708	10.756	11.307	71.16	3.196	.3147	1.0872	1.6939	.5869	.7282	.8107
3,400	138.98	10.271	10.446	11.573	12.014	82.01	3.362	.3025	1.0932	1.7903	.5422	.7141	.7821
3,600	156.18	10.637	11.057	12.250	12.721	91.50	3.529	.2946	1.0963	1.8453	.5147	.7098	.7636
3,800	170.65	10.816	11.551	12.798	13.428	99.48	3.706	.2882	1.0974	1.8702	.4994	.7146	.7482
4,000	181.92	10.834	11.928	13.215	14.134	105.80	3.858	.2854	1.0971	1.8691	.4941	.7213	.7419
4,200	191.88	10.798	12.213	13.531	14.841	111.49	3.981	.2841	1.0964	1.8596	.4924	.7251	.7391
4,400	201.68	10.763	12.566	13.922	15.548	117.10	4.059	.2876	1.0957	1.8507	.4913	.7216	.7488
4,600	212.28	10.766	12.894	14.286	16.254	123.18	4.128	.2901	1.0954	1.8483	.4886	.7157	.7559
4,800	225.06	10.833	13.273	14.706	16.961	130.23	4.197	.2914	1.0960	1.8602	.4819	.7074	.7600
5,000	240.24	11.010	13.705	15.184	17.668	138.65	4.281	.2908	1.0972	1.8839	.4716	.6993	.7591
5,500	294.36	11.785	15.127	16.760	19.435	168.48	4.526	.2836	1.1034	2.0070	.4277	.6715	.7420
6,000	379.31	13.045	17.101	18.947	21.201	214.57	4.875	.2689	1.1123	2.2114	.3668	.6412	.7052
6,500	496.72	14.460	19.497	21.601	22.968	277.87	5.313	.2538	1.1205	2.4418	.3068	.6140	.6670
7,000	634.15	15.611	21.974	24.346	24.735	352.49	5.819	.2419	1.1260	2.6288	.2608	.5975	.6366
7,500	767.45	16.260	24.144	26.750	26.502	424.83	6.315	.2351	1.1287	2.7332	.2319	.5907	.6193
8,000	873.84	16.405	25.758	28.538	28.269	482.75	6.782	.2315	1.1292	2.7548	.2175	.5949	.6102
8,500	947.86	16.200	26.839	29.736	30.035	524.31	-----	-----	1.1281	2.7191	.2130	-----	-----
9,000	1003.36	15.891	27.632	30.614	31.802	555.15	-----	-----	1.1266	2.6658	.2129	-----	-----
9,500	1051.30	15.572	28.304	31.359	33.569	581.93	-----	-----	1.1250	2.6116	.2142	-----	-----
10,000	1097.98	15.274	28.946	32.070	35.336	609.11	-----	-----	1.1235	2.5609	.2156	-----	-----
11,000	1216.15	14.950	30.488	33.778	38.869	674.53	-----	-----	1.1216	2.5051	.2139	-----	-----
H = 173,885 ft; $T_1 = 283^\circ$ K; $p_1 = 0.5756 \times 10^{-3}$ atm.													
2,000	43.78	6.185	6.035	$6.686 \times 10^3$	7.067	29.35	-----	-----	1.0343	1.1724	0.8808	-----	-----
2,200	50.82	6.510	6.482	7.182	7.774	33.35	-----	-----	1.0403	1.2140	.8533	-----	-----
2,400	59.68	6.961	6.993	7.748	8.481	38.35	-----	-----	1.0489	1.2787	.8114	-----	-----
2,600	71.72	7.617	7.623	8.446	9.187	45.01	-----	-----	1.0606	1.3788	.7506	-----	-----
2,800	87.70	8.456	8.378	9.282	9.894	53.85	-----	-----	1.0732	1.5098	.6782	-----	-----
3,000	107.35	9.374	9.218	10.213	10.676	64.56	3.055	0.3215	1.0847	1.6542	.6113	0.7320	0.8260
3,200	128.39	10.171	10.042	11.126	11.307	76.09	3.224	.3062	1.0928	1.7792	.5502	.7112	.7902
3,400	148.59	10.704	10.780	11.943	12.014	86.78	3.406	.2953	1.0974	1.8607	.5104	.7020	.7646
3,600	163.48	10.954	11.297	12.516	12.721	95.46	3.588	.2875	1.0992	1.8972	.4938	.7069	.7458
3,800	175.73	11.009	11.712	12.976	13.428	102.32	3.760	.2830	1.0992	1.9017	.4862	.7154	.7351
4,000	185.55	10.956	12.040	13.339	14.134	107.94	3.883	.2831	1.0982	1.8890	.4847	.7194	.7361
4,200	195.05	10.902	12.349	13.682	14.841	113.33	3.981	.2845	1.0974	1.8766	.4846	.7197	.7403
4,400	205.32	10.889	12.672	14.040	15.548	119.15	4.050	.2874	1.0969	1.8713	.4833	.7140	.7484
4,600	217.25	10.917	13.035	14.442	16.254	125.88	4.114	.2899	1.0968	1.8730	.4783	.7056	.7557
4,800	232.02	11.092	13.462	14.915	16.961	134.04	4.187	.2899	1.0982	1.8996	.4687	.6961	.7567
5,000	250.35	11.342	13.971	15.479	17.668	144.16	4.270	.2885	1.1002	1.9387	.4542	.6846	.7537
5,500	318.45	12.457	15.696	17.390	19.435	181.13	4.553	.2767	1.1086	2.1183	.3979	.6514	.7247
6,000	423.47	14.003	18.021	19.966	21.201	238.16	4.964	.2593	1.1182	2.3697	.3308	.6200	.6808
6,500	561.50	15.521	20.679	22.911	22.968	312.58	5.456	.2442	1.1259	2.6170	.2731	.5950	.6423
7,000	709.17	16.544	23.195	25.698	24.735	392.30	5.986	.2342	1.1302	2.7830	.2343	.5826	.6168
7,500	832.52	16.888	25.117	27.828	26.502	459.94	6.487	.2293	1.1314	2.8369	.2144	.5835	.6042
8,000	918.87	16.771	26.395	29.244	28.249	507.15	-----	-----	1.1307	2.8152	.2071	-----	-----
8,500	977.24	16.424	27.240	30.180	30.035	539.84	-----	-----	1.1291	2.7558	.2068	-----	-----
9,000	1023.63	16.034	27.901	30.912	31.802	566.59	-----	-----	1.1273	2.6903	.2088	-----	-----
9,500	1071.93	15.727	28.571	31.655	33.569	593.26	-----	-----	1.1257	2.6372	.2102	-----	-----
10,000	1126.13	15.496	29.300	32.462	35.336	623.39	-----	-----	1.1245	2.5976	.2105	-----	-----
11,000	1266.51	15.273	31.090	34.445	38.869	702.48	-----	-----	1.1233	2.5587	.2058	-----	-----

TABLE II.- HYPERSONIC NORMAL-SHOCK PARAMETERS AT SIX SELECTED ALTITUDES - Concluded

$T_2$ , °K	$\frac{p_2}{p_1}$	$\frac{\rho_2}{\rho_1}$	$M_1$	$u_1$ , ft	$\frac{T_2}{T_1}$	$\frac{h_2}{R} \frac{1}{T_0}$	$\frac{a_2}{a_1}$	$M_2$	$K_{p2}$	$K_{\rho 2}$	$K_{T2}$	$K_{a2}$	$K_{M2}$
H = 246,060 ft; $T_1 = 197^\circ$ K; $p_1 = 0.2420 \times 10^{-4}$ atm.													
2,000	67.23	6.593	7.465	$6.897 \times 10^3$	10.152	29.97	-----	-----	1.0368	1.1974	0.8620	-----	-----
2,200	81.53	7.183	8.172	7.550	11.168	35.55	-----	-----	1.0487	1.2868	.8019	-----	-----
2,400	103.82	8.208	9.142	8.446	12.183	44.07	-----	-----	1.0666	1.4499	.7086	-----	-----
2,600	135.95	9.581	10.371	9.581	13.198	56.24	-----	-----	1.0849	1.6711	.6039	-----	-----
2,800	173.55	10.869	11.647	10.760	14.213	70.46	-----	-----	1.0978	1.8783	.5203	-----	-----
3,000	206.74	11.650	12.674	11.709	15.228	83.14	3.850	0.2825	1.1041	2.0021	.4732	0.6790	0.7360
3,200	229.96	11.910	13.357	12.340	16.244	91.89	4.096	.2738	1.1057	2.0406	.4559	.6862	.7141
3,400	244.88	11.810	13.790	12.740	17.259	97.83	4.314	.2707	1.1045	2.0201	.4551	.7006	.7068
3,600	257.03	11.648	14.139	13.062	18.274	102.73	4.468	.2717	1.1028	1.9898	.4590	.7080	.7098
3,800	269.55	11.523	14.488	13.385	19.289	107.74	4.550	.2763	1.1015	1.9662	.4619	.7041	.7222
4,000	284.46	11.489	14.887	13.753	20.305	113.70	4.621	.2804	1.1009	1.9581	.4611	.6963	.7335
4,200	304.54	11.614	15.397	14.225	21.320	121.37	4.686	.2829	1.1017	1.9765	.4532	.6832	.7406
4,400	331.61	11.913	16.050	14.828	22.335	131.71	4.774	.2822	1.1040	2.0257	.4376	.6683	.7393
4,600	369.09	12.433	16.903	15.616	23.350	145.78	4.904	.2773	1.1078	2.1084	.4133	.6524	.7274
4,800	418.60	13.145	17.962	16.594	24.366	164.49	5.057	.2702	1.1127	2.2248	.3827	.6337	.7092
5,000	482.44	14.032	19.236	17.771	25.381	188.47	5.246	.2613	1.1180	2.3703	.3482	.6144	.6865
5,500	703.72	16.518	23.106	21.347	27.919	271.48	5.864	.2385	1.1301	2.7787	.2665	.5730	.6280
6,000	973.55	18.426	27.093	25.030	30.457	371.79	6.589	.2232	1.1371	3.0919	.2120	.5497	.5885
6,500	1185.12	18.969	29.870	27.595	32.995	451.81	7.214	.2183	1.1387	3.1792	.1892	.5462	.5758
7,000	1301.24	18.605	31.318	28.933	35.533	496.59	-----	-----	1.1374	3.1166	.1854	-----	-----
7,500	1370.66	18.006	32.173	29.723	38.071	523.71	-----	-----	1.1351	3.0154	.1883	-----	-----
8,000	1434.92	17.486	32.948	30.439	40.609	548.29	-----	-----	1.1331	2.9278	.1915	-----	-----
8,500	1505.79	17.049	33.779	31.207	43.147	577.86	-----	-----	1.1313	2.8539	.1937	-----	-----
9,000	1611.57	16.915	34.955	32.293	45.685	616.69	-----	-----	1.1307	2.8307	.1915	-----	-----
9,500	1747.11	16.911	36.396	33.625	48.223	668.79	-----	-----	1.1306	2.8292	.1865	-----	-----
10,000	1928.51	17.101	38.227	35.316	50.761	736.97	-----	-----	1.1313	2.8610	.1781	-----	-----
11,000	2433.88	17.740	42.898	39.631	55.838	928.96	-----	-----	1.1337	2.9648	.1556	-----	-----
H = 295,280 ft; $T_1 = 197^\circ$ K; $p_1 = 0.1792 \times 10^{-5}$ atm.													
2,000	72.88	7.082	7.729	$7.140 \times 10^3$	10.152	32.04	-----	-----	1.0481	1.2791	0.8084	-----	-----
2,200	98.83	8.488	8.897	8.220	11.168	41.94	-----	-----	1.0721	1.5041	.6837	-----	-----
2,400	139.56	10.459	10.458	9.662	12.183	57.16	-----	-----	1.0953	1.8228	.5486	-----	-----
2,600	183.48	12.041	11.918	11.010	13.198	73.80	-----	-----	1.1083	2.0775	.4621	-----	-----
2,800	213.73	12.628	12.841	11.863	14.213	85.18	-----	-----	1.1119	2.1684	.4306	-----	-----
3,000	229.52	12.501	13.315	12.301	15.228	91.46	4.067	0.2619	1.1105	2.1422	.4299	0.6833	0.6833
3,200	241.13	12.273	13.660	12.620	16.244	96.05	4.249	.2623	1.1085	2.1004	.4363	.6965	.6847
3,400	252.29	12.050	13.986	12.921	17.259	100.57	4.320	.2687	1.1064	2.0596	.4434	.6925	.7017
3,600	266.18	11.953	14.372	13.278	18.274	106.12	4.373	.2750	1.1053	2.0403	.4445	.6821	.7188
3,800	286.50	12.086	14.905	13.770	19.289	113.78	4.435	.2781	1.1060	2.0596	.4370	.6674	.7274
4,000	316.41	12.489	15.644	14.453	20.305	125.12	4.526	.2767	1.1089	2.1241	.4184	.6498	.7245
4,200	360.27	13.212	16.656	15.388	21.320	141.88	4.662	.2704	1.1136	2.2416	.3884	.6293	.7088
4,400	424.16	14.315	18.020	16.648	22.335	165.69	4.845	.2598	1.1201	2.4226	.3486	.6052	.6821
4,600	510.38	15.691	19.706	18.205	23.350	197.66	5.081	.2472	1.1269	2.6488	.3054	.5810	.6497
4,800	619.70	17.194	21.654	20.005	24.366	238.23	5.352	.2353	1.1332	2.8962	.2645	.5576	.6192
5,000	745.54	18.584	23.699	21.894	25.381	285.58	5.664	.2251	1.1381	3.1249	.2304	.5397	.5928
5,500	1059.71	20.759	28.177	26.031	27.919	402.58	-----	-----	1.1443	3.4817	.1798	-----	-----
6,000	1234.65	20.708	30.416	28.100	30.457	468.91	-----	-----	1.1441	3.4700	.1684	-----	-----
6,500	1309.71	19.696	31.370	28.981	32.995	497.64	-----	-----	1.1409	3.2993	.1716	-----	-----
7,000	1366.07	19.070	32.067	29.625	35.533	520.62	-----	-----	1.1389	3.1937	.1769	-----	-----
7,500	1439.73	18.519	32.948	30.439	38.071	549.65	-----	-----	1.1370	3.1008	.1796	-----	-----
8,000	1555.53	18.345	34.257	31.648	40.609	592.86	-----	-----	1.1363	3.0705	.1772	-----	-----
8,500	1728.80	18.510	36.107	33.358	43.147	657.88	-----	-----	1.1368	3.0968	.1696	-----	-----
9,000	1973.21	18.966	38.550	35.615	45.685	751.10	-----	-----	1.1382	3.1715	.1576	-----	-----
9,500	2306.36	19.576	41.642	38.471	48.223	876.46	-----	-----	1.1401	3.2722	.1426	-----	-----
10,000	2725.45	20.275	45.228	41.784	50.761	1033.05	-----	-----	1.1421	3.3873	.1273	-----	-----
11,000	3716.52	21.215	52.757	48.740	55.838	1405.64	-----	-----	1.1446	3.5422	.1030	-----	-----

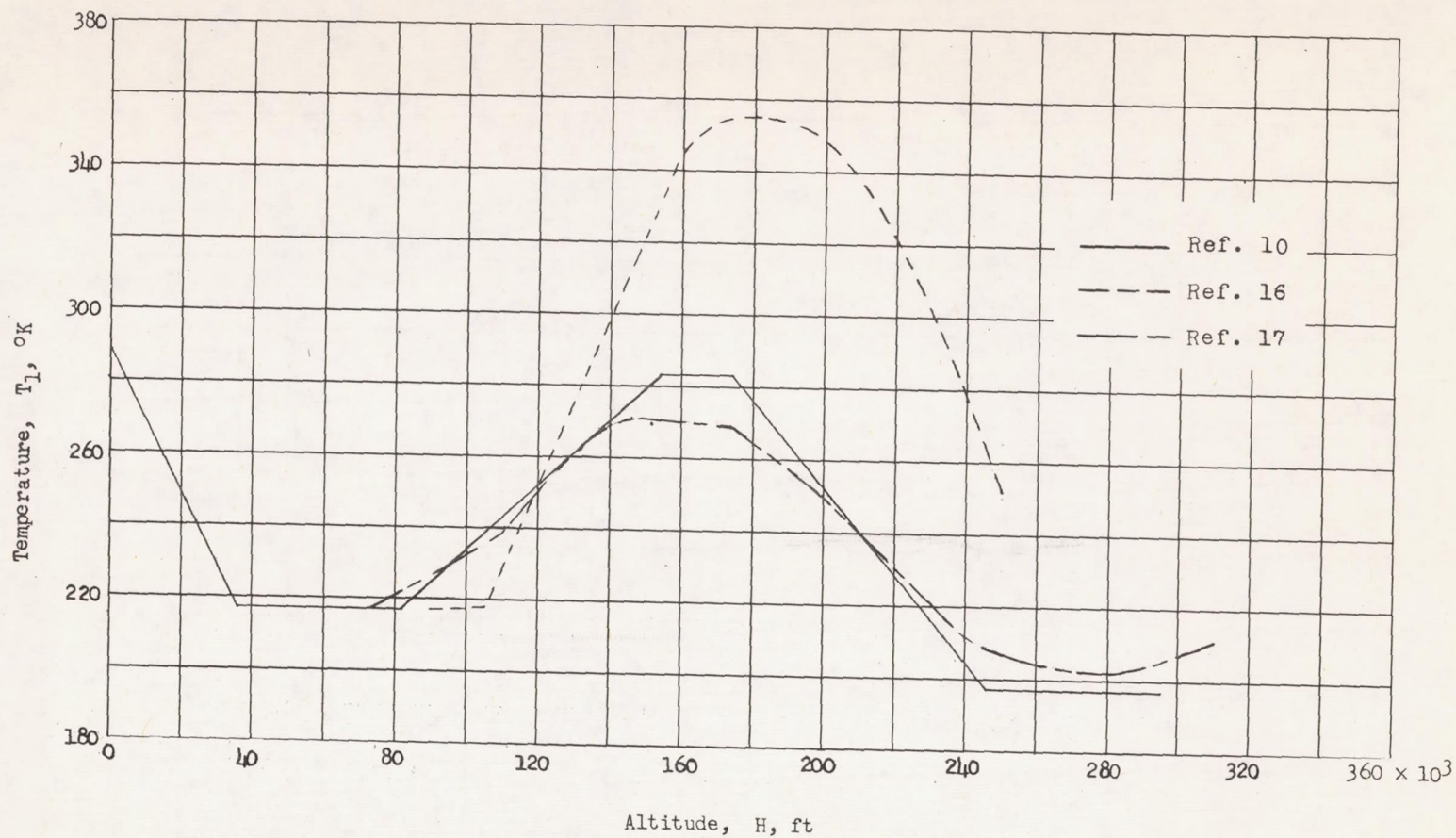


Figure 1.- Variation of atmospheric temperature with altitude.

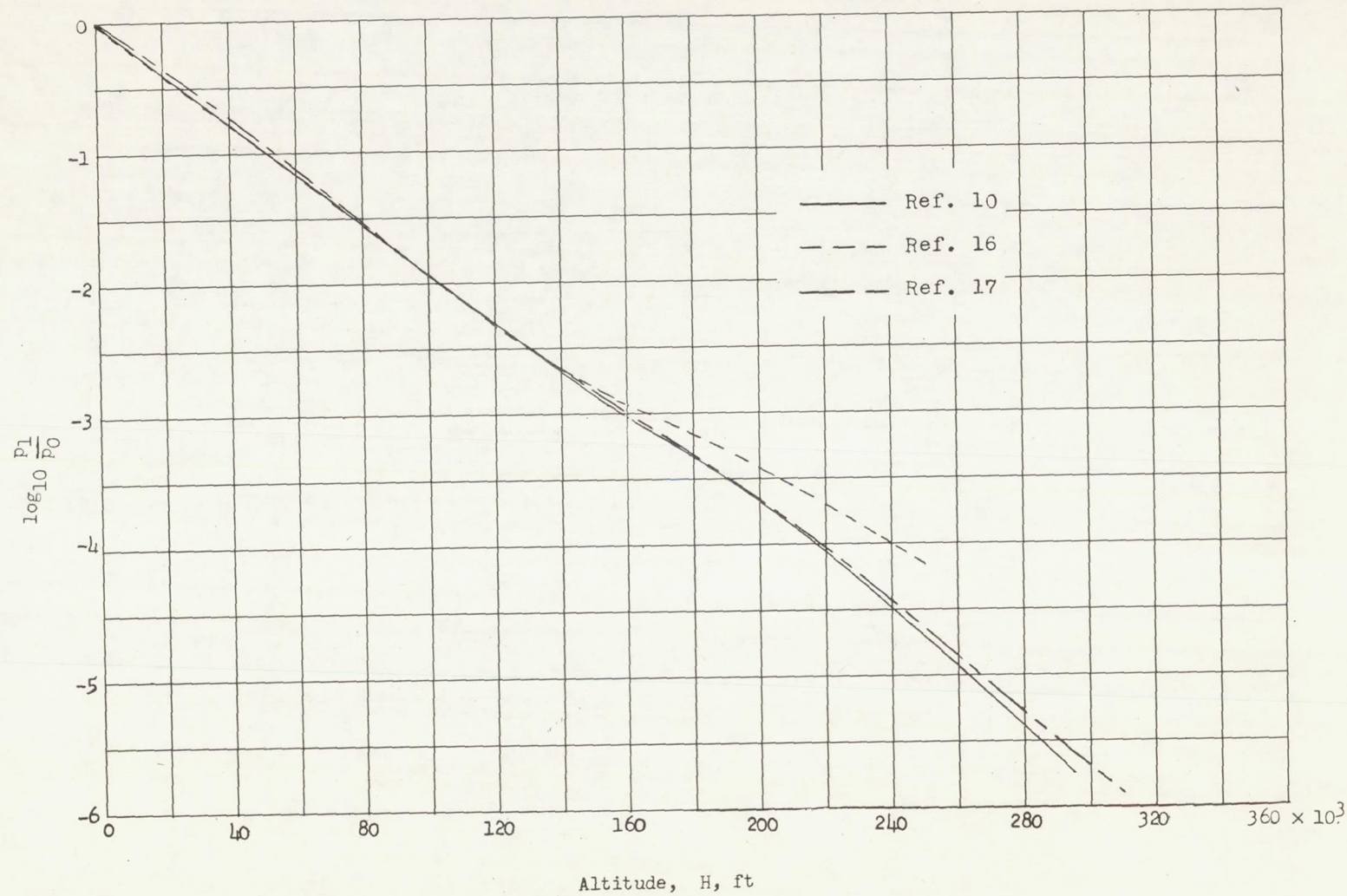


Figure 2.- Variation of atmospheric pressure with altitude.

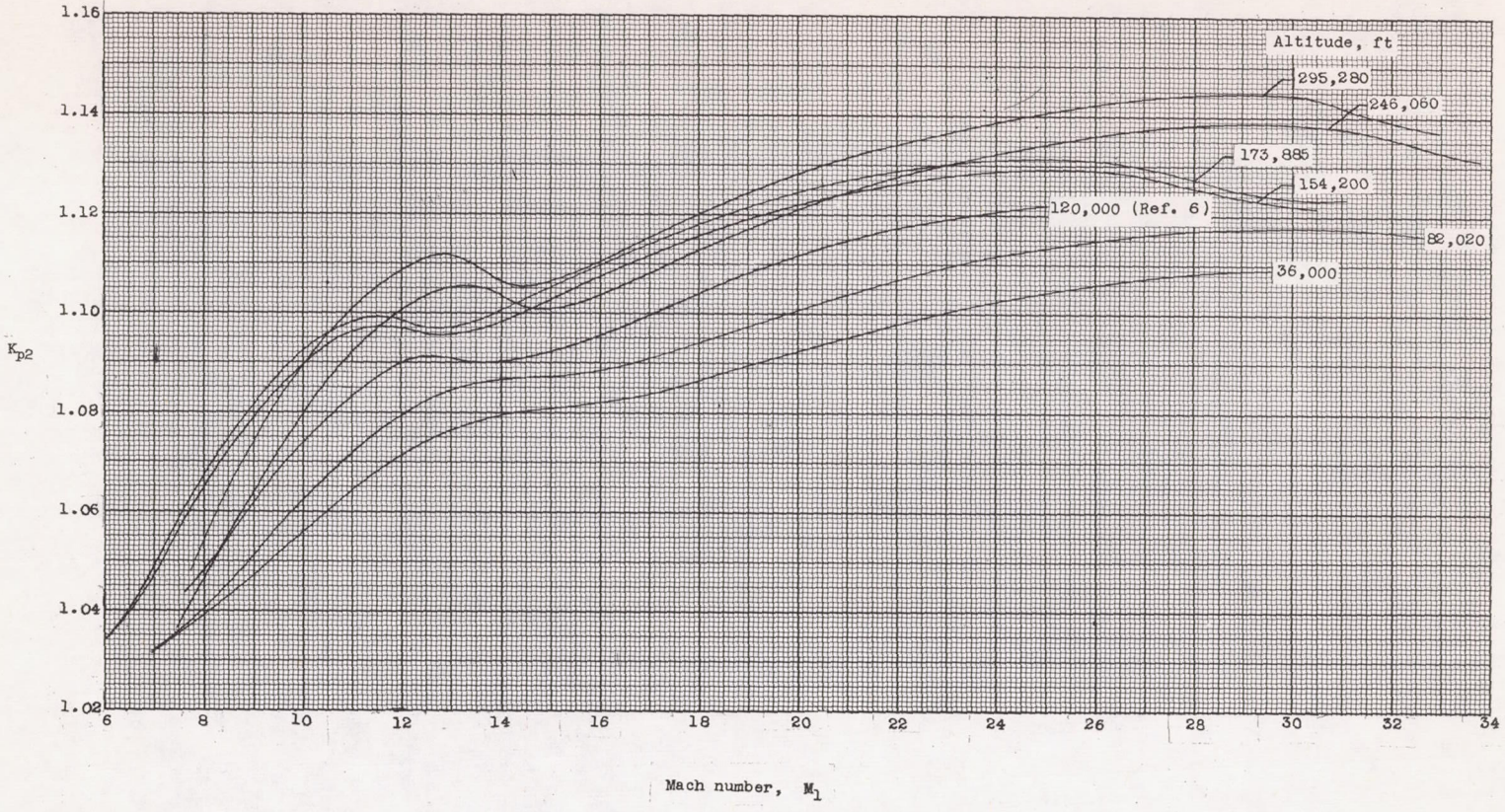


Figure 3.- Variation with Mach number and altitude of the ratio of real to ideal values of normal-shock pressure ratio.

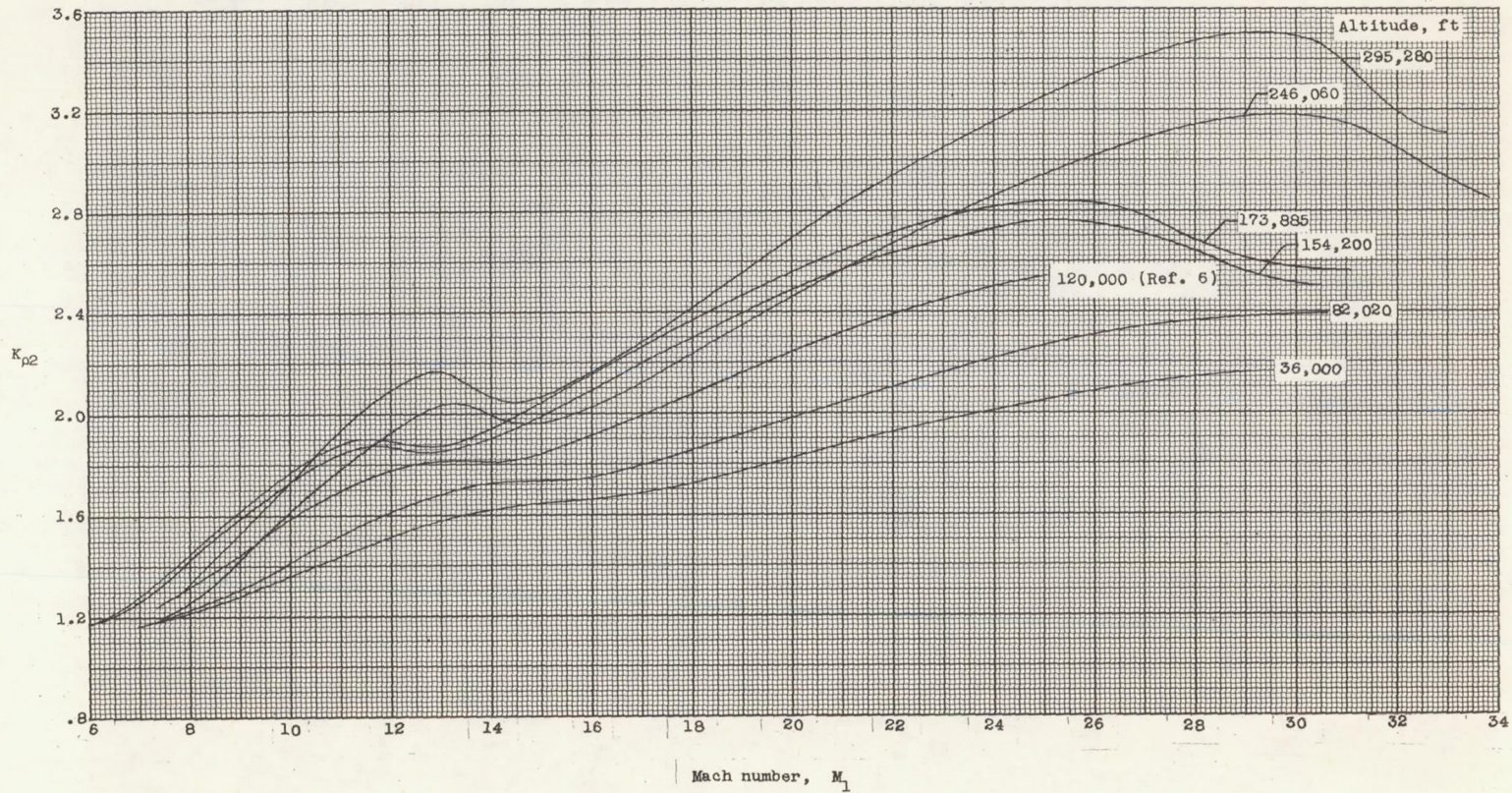


Figure 4.- Variation with Mach number and altitude of the ratio of real to ideal values of normal-shock density ratio.

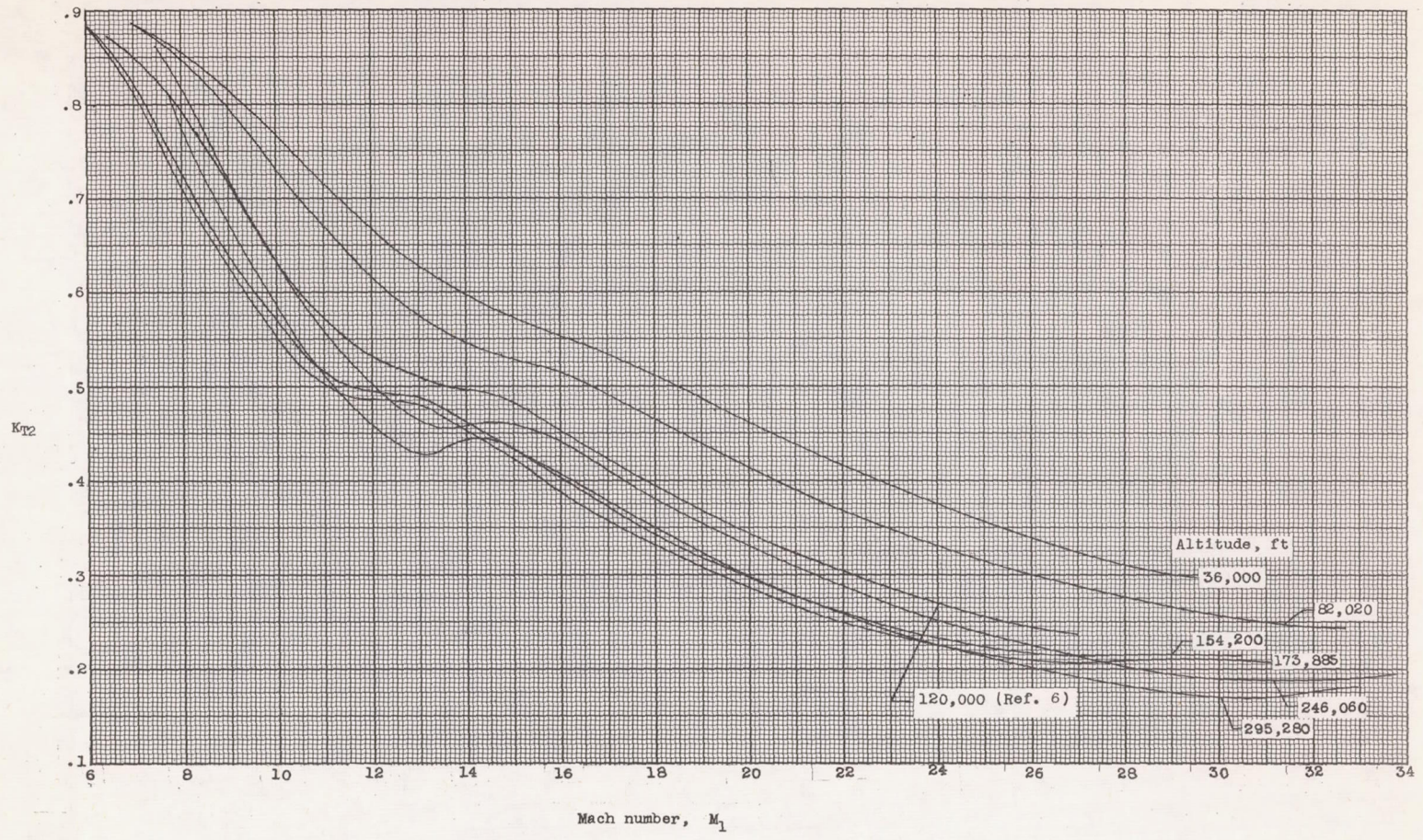


Figure 5.- Variation with Mach number and altitude of the ratio of real to ideal values of normal-shock temperature ratio.

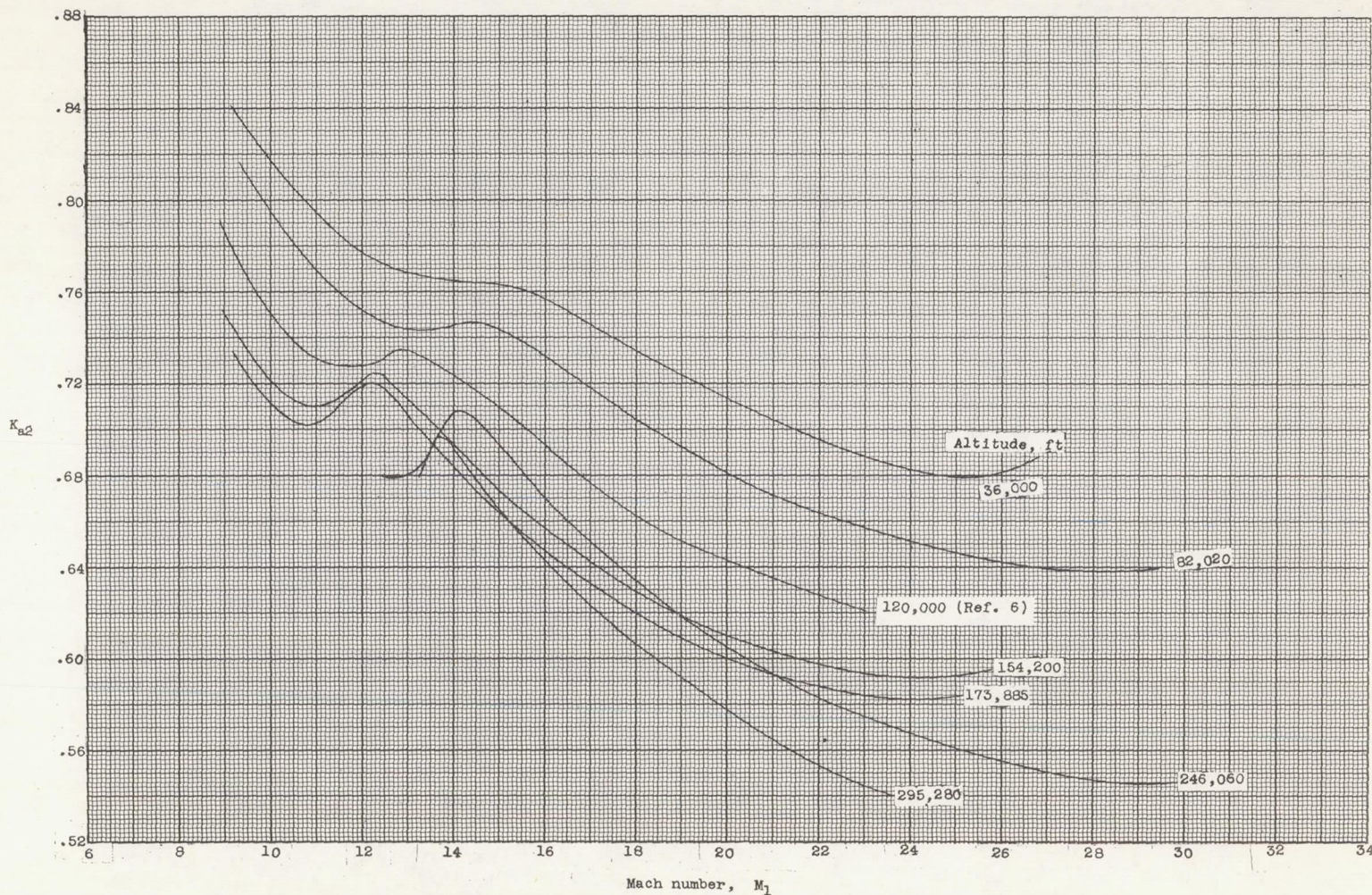


Figure 6.- Variation with Mach number and altitude of the ratio of real to ideal values of normal-shock velocity-of-sound ratio.



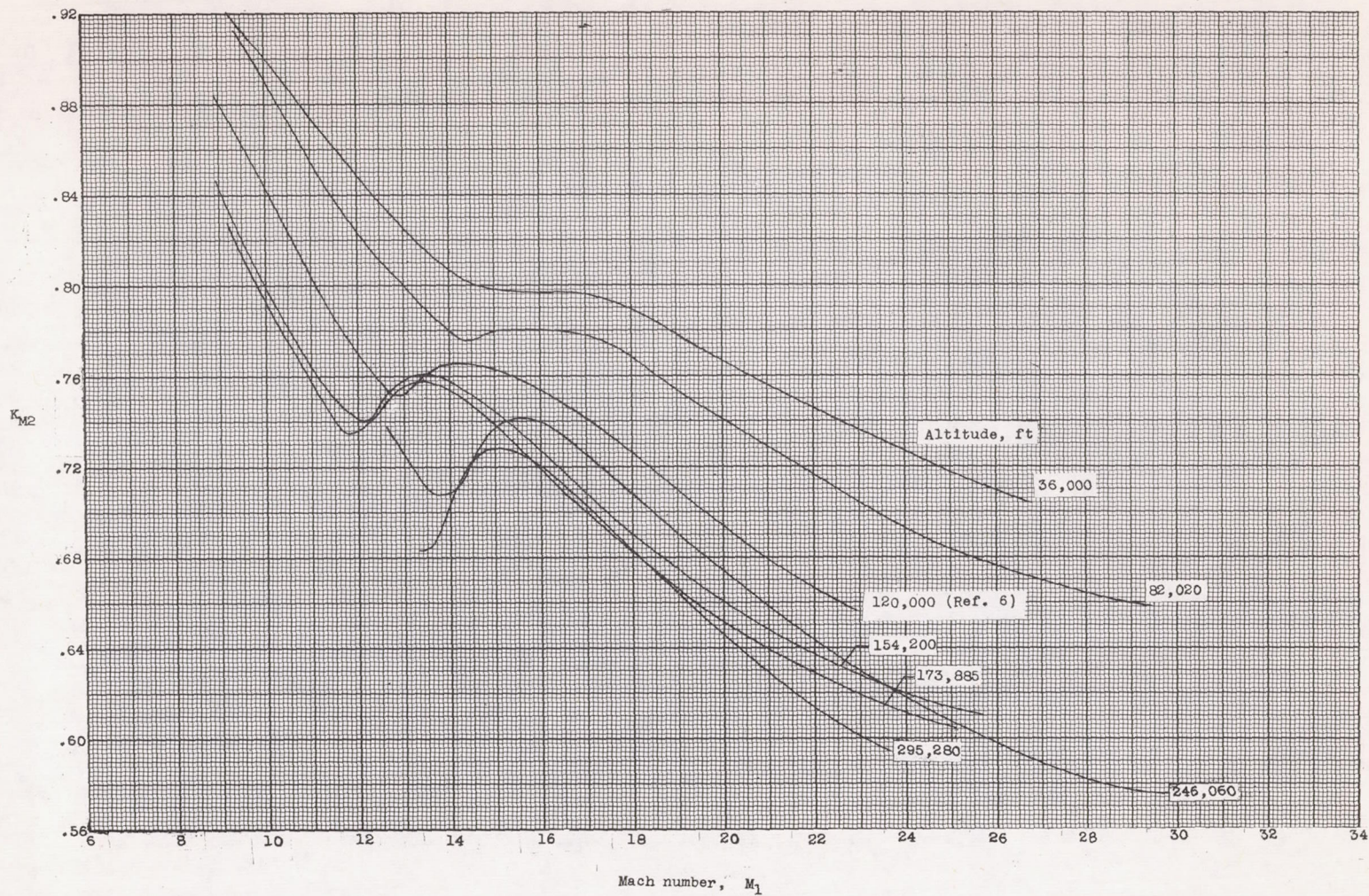


Figure 7.- Variation with Mach number and altitude of the ratio of real to ideal values of Mach number behind normal shock.

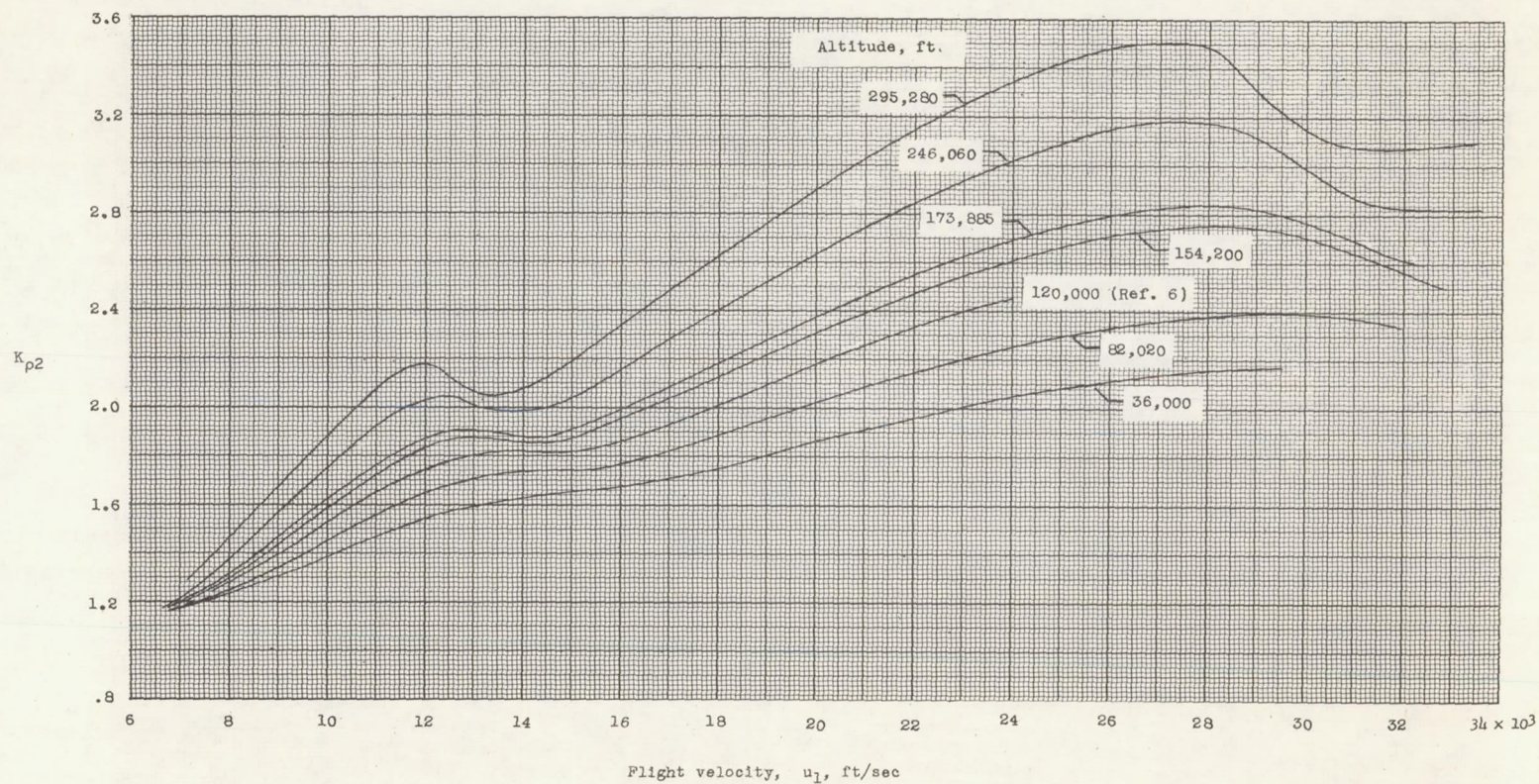


Figure 8.- Variation with flight velocity and altitude of the ratio of real to ideal values of normal shock density ratio.

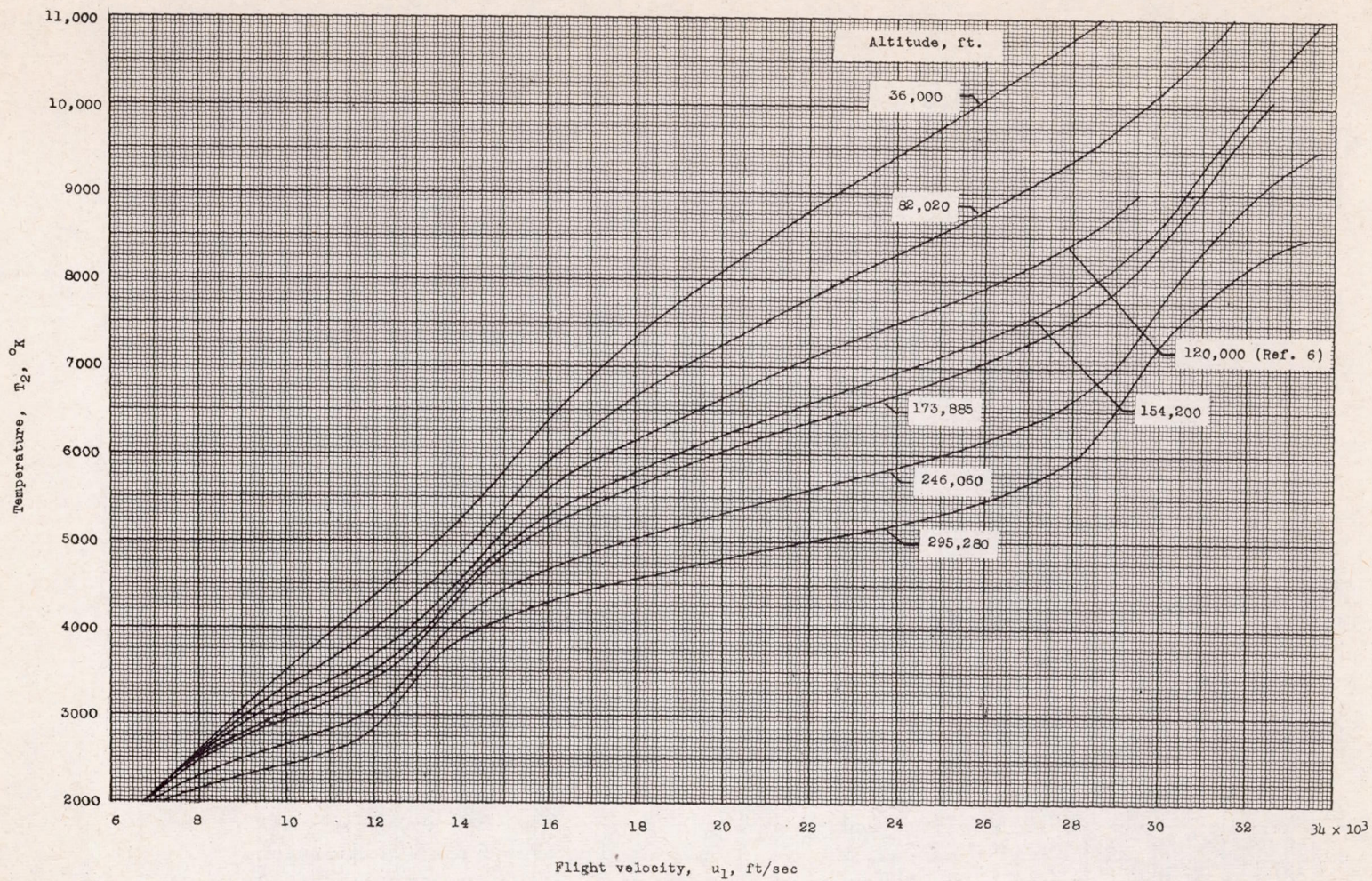


Figure 9.- Variation with flight velocity and altitude of the temperature behind a normal shock.

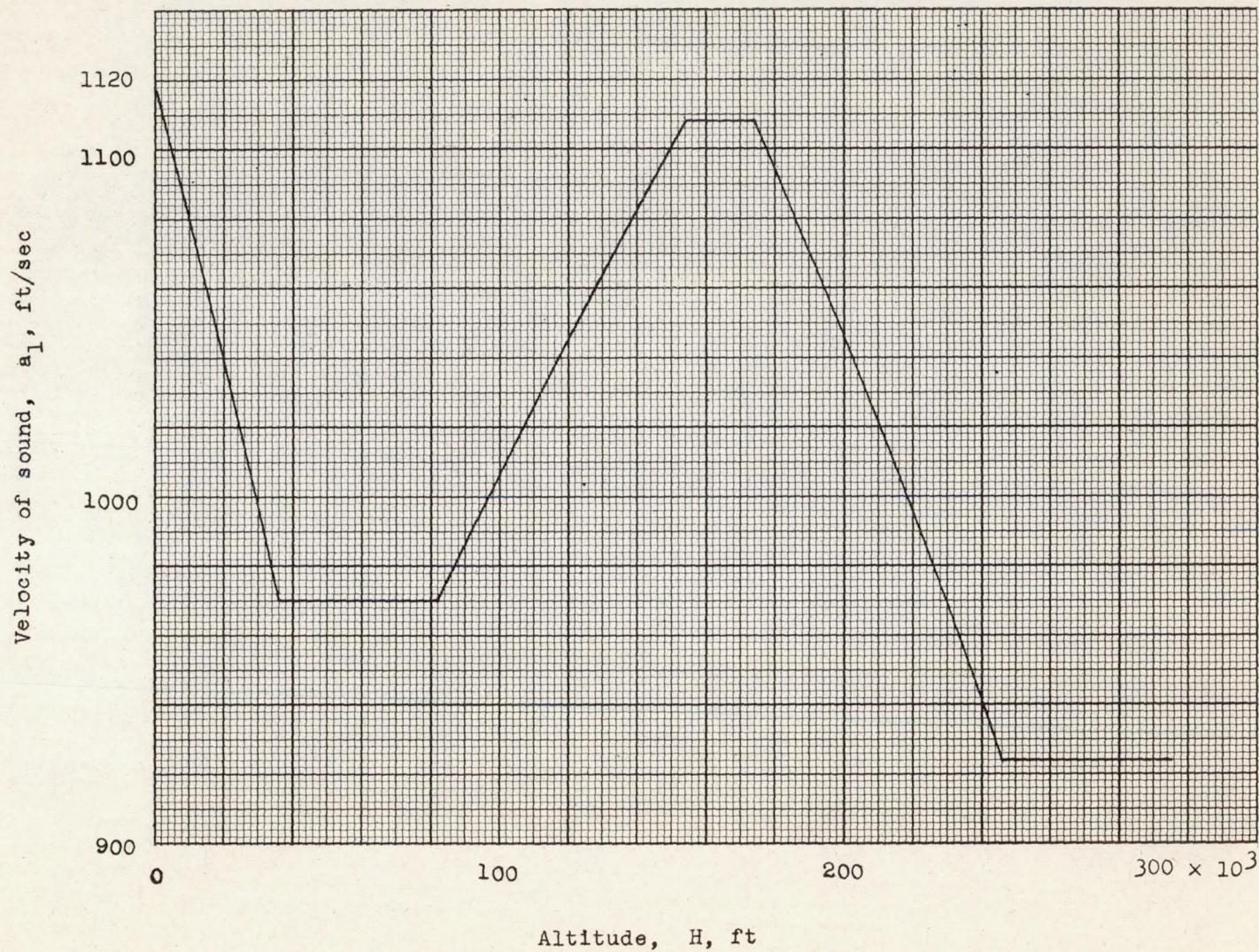


Figure 10.- Variation of velocity of sound with altitude for an argon-free model atmosphere.